Inactive CONFIDENTIAL Copy 6
RM L50I06

NACA RM L50I06

3 1176 00149 9376

MAR 22 1951

NACA

RESEARCH MEMORANDUM

STRAIN-GAGE MEASUREMENTS OF BUFFETING LOADS

ON A JET-POWERED BOMBER AIRPLANE

By William S. Aiken, Jr. and John A. See

Langley Aeronautical Laboratory
Langley Field, Va.

CLASSIFICATION CANCELLED

Authority NACA R7 2983 Date 4/14/55

By MHA 5/3/55 See

CLASSIFIED DOCUMENT

NATIONAL ADVISORY COMMITTEE
FOR AERONAUTICS
WASHINGTON
March 19, 1951

CONFIDENTIAL

NATIONAL ADVISORY COMMITTEE FOR AERONAUTICS

RESEARCH MEMORANDUM

STRAIN-GAGE MEASUREMENTS OF BUFFETING LOADS ON A JET-POWERED BOMBER AIRPLANE

By William S. Aiken, Jr. and John A. See

SUMMARY

Buffet boundaries, buffeting-load increments for the stabilizers and elevators, and buffeting bending-moment increments for the stabilizers and wings as measured in gradual maneuvers for a jet-powered bomber airplane are presented. The buffeting-load increments were determined from strain-gage measurements at the roots or hinge supports of the various surfaces considered. The Mach numbers of the tests ranged from 0.19 to 0.78 at altitudes close to 30,000 feet. The predominant buffet frequencies were close to the natural frequencies of the structural components. The buffeting-load data, when extrapolated to low-altitude conditions, indicated loads on the elevators and stabilizers near the design limit loads. When the airplane was held in buffeting, the load increments were larger than when recovery was made immediately.

INTRODUCTION

The NACA is currently conducting a flight investigation of a B-45A airplane with the primary objectives of checking the accuracy of available methods of computing loads and load distributions on the horizontal tail of a jet-bomber airplane, and obtaining full-scale data on the zero-lift pitching-moment coefficient and aerodynamic center of the wing-fuselage combination.

The results of some of these tests have been reported in time-history form in references 1 to 5. During the course of these tests buffeting was encountered at several combinations of Mach number and airplane normal-force coefficient. To better define safe operating limits as the tests progressed to lower altitudes, an additional flight was made at high altitude with the particular object of obtaining buffet data. From these limited data it was possible to define a buffet boundary and to estimate the magnitudes of loads on the elevators, stabilizers, and wings for lower altitudes. These data, which are presented in this paper, all apply to the original B-45A configuration, that is, without reflexed flaps and ailerons and tail-tip incidence changes.

SYMBOLS

C_N	normal-force coefficient $\left(\frac{\text{Load}}{qS}\right)$
C_{BM}	bending-moment coefficient $\left(\frac{\text{Bending moment}}{qS\frac{b}{2}}\right)$
q	dynamic pressure, pounds per square foot $\left(0.7pM^2\right)$
p	free-stream static pressure, pounds per square foot
M	Mach number
S	area of component being considered, square feet
b/2	semispan of component being considered, inches
n	airplane normal acceleration, g units
BM	bending moment, inch-pounds

Subscripts:

A	airplane
T	horizontal tail
E	elevator
W	wing
B	buffet

TESTS AND INSTRUMENTATION

All tests reported in this paper were made with the original B-45A service configuration, that is, without the reflexed flaps and ailerons or changes in the stabilizer tip incidence which are now incorporated on all B-45A airplanes. (Table I gives some pertinent geometric characteristics of the airplane.)

The test data fall into two classes, intentional buffeting and inadvertent buffeting for the airplane in the clean condition. All data obtained in intentional-buffeting maneuvers were from one flight, which was made for the purpose of establishing the airplane buffet boundary in gradual turning maneuvers. Fourteen turns were made at Mach numbers from 0.48 to 0.78 at a pressure altitude close to 30,000 feet, and on eight of these runs buffeting-load data were obtained. For six of the fourteen runs it was not possible to obtain buffeting without exceeding 3.0g (the maximum load factor set for these tests).

Some 22 runs from other flights where buffeting was encountered are also included in the data. These runs include wind-up turns, level-flight stalls, and abrupt pull-ups. Most of these data were also obtained in the vicinity of 30,000 feet pressure altitude.

The primary load-measuring instrumentation for determining buffeting loads consisted of shear and bending-moment measuring strain-gage bridges mounted on the main spars of the wing and tail surfaces. Loads on the elevator were measured by means of strain gages mounted on the individual hinge brackets. Figure 1 is a three-view drawing of the test airplane showing the approximate locations of the strain-gage bridges.

All strain-gage installations were initially calibrated in terms of the principal type of load affecting the output of the bridge. For example, to measure the shear at the root of the horizontal tail on one side, four arm shear strain-gage bridges were mounted on the webs of the three main stabilizer spars. Calibrating loads were first applied to the structure outboard of the strain-gage station in order to determine the responses from the individual bridges. These bridges were then combined electrically so that the shear independent of torque could be evaluated from the recording of only one channel. Following the electrical combination of the shear strain-gage bridges, the tail was recalibrated to determine the effects of bending moment and carry-through on the measured shear deflection. Thus, the net shear of either side of the tail was assumed to be given by an equation of the form

$$\text{Net Shear} = A\delta_{S_L} + B\delta_{BM_L} + C\delta_{BM_R}$$

where A, B, and C are calibration coefficients and the δ symbols refer to strain-gage deflections for left shear, left bending moment, and right bending moment, respectively. The term $A\delta_{S_L}$ is the primary term in computing the shear and the other terms are merely corrections. The actual equations which were used to determine net tail loads are

$$\text{Net Shear (Left Tail)} = 6840\delta_{S_L} + 300\delta_{BM_L} + 670\delta_{BM_R}$$

$$\text{Net Shear (Right Tail)} = 4760\delta_{S_R} + 640\delta_{BM_R} + 660\delta_{BM_L}$$

where the δ's refer to the ratio of strain-gage deflection to calibrate signal deflection. For the determination of aerodynamic loads, an inertia correction is added to the net shears.

All of this is mentioned in detail to point out that, for the buffeting incremental loads given in this paper, only the portion of the shear measured by use of the primary term $A\delta_S$ is used. In evaluating strain records of rapidly oscillating loads by using more than one strain-gage record large errors would be introduced due to difficulties in exact time correlation since the shears and bending moments are not always in phase. The shear given by the term $A\delta_S$ is the major portion of the structural shear (aerodynamic plus inertia) at the strain gage station. The other terms ($B\delta_{BM_L}$ and $C\delta_{BM_R}$) are used to obtain accurate measurements of non-buffeting loads.

The bending moment on the horizontal stabilizers was determined in a manner similar to the shear, different calibration constants being used in the equations. Shear and bending moment at the root of both wings were also found in the same manner.

The elevator loads were measured by combining the output from the three outer hinge-support strain-gage bridges and the three inner hinge-support strain-gage bridges and then determining the elevator load from a calibration equation of the form

$$\text{Net Load (Elevator)} = A\delta_{out} + B\delta_{in}$$

The actual equations used for determining the elevator net loads were

$$\text{Net Load (Left Elevator)} = 2650\delta_{out} + 5370\delta_{in}$$

$$\text{Net Load (Right Elevator)} = 2940\delta_{out} + 4470\delta_{in}$$

The various strain-gage deflections were recorded on two 18-channel Consolidated oscillographs at paper speeds from 2 to 4 inches per second with individual galvanometer responses linear to 60 cycles per second.

Standard NACA photographic recording instruments installed for the primary test program were used to measure airspeed and altitude, rolling, pitching, and yawing velocities, sideslip angle, accelerations, control forces, and control positions. Normal, transverse, and longitudinal accelerations were measured at the airplane center of gravity and at fuselage station 714 (approx. the one-quarter mean chord of the horizontal tail).

An airspeed boom was mounted at the left wing tip with the airspeed head approximately one local chord length ahead of the leading edge. The results of a flight calibration of the airspeed system for position error and an analysis of available data for a similar installation indicate the measured Mach number differs from the true Mach number by less than ±0.01 throughout the test range.

RESULTS AND DISCUSSION

Buffet Boundary

For the tests where the pilot was intentionally approaching buffeting conditions a switch was provided which, when depressed, marked an accelerometer record. The pilot's opinion of the start of buffeting could then be correlated with either strain-gage or accelerometer records. It was found that the pilot was sensitive to an oscillating load of ±200-pounds-per-side change in tail or stabilizer load so that this criterion was used to establish a gradual-stall buffet boundary for the original service configuration.

Figure 2 is a sample oscillograph record showing the approach to buffeting and the manner in which the intensity of buffeting increases with time under buffeting conditions. The maneuver shown is a gradual turn at a Mach number of 0.72 at an altitude of 33,500 feet. For simplicity, only a few of the traces are identified. They are as follows:

1. Left-stabilizer shear
2. Right-stabilizer shear
3. Left-stabilizer bending
4. Left-wing bending
5. Left-elevator outboard shear
6. Left-elevator inboard shear

For the sample record trace number 2, the right-stabilizer shear reaches a buffet amplitude of ±200 pounds at a time somewhere between 0.2 and 0.4 second. The actual trace deflection is shown in figure 2 as the shaded region labeled "±200 lbs." The pilot indicated the start of buffeting at time 0.2 second. The Mach number for the start of buffeting is 0.728 and the normal-force coefficient for the airplane, C_{N_A}, is 0.71.

The gradual-turn buffet boundary for the test airplane is shown in figure 3 in terms of C_{N_A} and Mach number for start of buffeting. All points shown on figure 3 were obtained at a pressure altitude of 30,000 feet with the exception of the point at $M = 0.23$ and $C_{N_A} = 1.34$ which was obtained from a level-flight stall at 17,000 feet. In addition to actual buffeting points, several maneuvers were made which closely approached the buffet boundary and a few of these have been used in order to aid in the determination of the boundary. All points where buffeting either stopped or started were established by the criterion of ±200 pounds tail load per side, illustrated in figure 2. For the airplane in the clean condition, in gradual turns or level-flight stall maneuvers, the points shown as circles indicate the start of buffeting, those as circles with crosses superimposed, the stop of buffeting, and the crosses, no buffet. The square points define a buffet boundary for abrupt pull-ups over a limited Mach number range.

Several points of interest may be noted in connection with figure 3. The boundary for the airplane in the clean condition, as defined by the solid line, is markedly similar to other buffet boundaries for airplanes having laminar flow or low-drag wings with a depression occurring near a Mach number of 0.5 and a secondary peak around a Mach number of 0.65 followed by a sharp drop toward zero airplane normal-force coefficient. The points which define the boundary are quite consistent except at the lowest Mach numbers.

The three abrupt pull-up points at Mach numbers of 0.355, 0.402, and 0.452 show the expected increase in maximum normal-force coefficient with pitching velocity before buffeting is reached.

Buffeting boundaries were calculated from the faired curve of figure 3 and are shown in figure 4 for various altitudes. The curves given apply to the clean condition and a weight of 82,600 pounds. Under these conditions figure 4 indicates that buffeting would not be encountered without exceeding the design load factor of 3.0g under the following approximate conditions:

1. Pressure altitude - 0 feet, no buffeting between Mach numbers of 0.40 and 0.76

2. Pressure altitude - 10,000 feet, no buffeting between Mach numbers of 0.52 and 0.75

3. Pressure altitude - 20,000 feet, no buffeting between Mach numbers 0.60 and 0.74

At altitudes above about 28,000 feet, buffeting may be encountered without exceeding 3.0g. From figure 4 it may also be noted that buffeting will be encountered in level flight at a Mach number of 0.75 at a pressure altitude of 40,000 feet.

Buffeting-Load Increments

Horizontal stabilizer shear.- As described under the section entitled "Instrumentation," the buffeting increments given for horizontal stabilizer shear were obtained from the strain-gage records by considering only the portion of the shear measured by the combined shear gages. Because torsional effects have been calibrated out, the buffeting-load increments are not representative of the stresses in the individual spars. The maximum buffeting increment about a mean curve through the time-history record was determined for each run where buffeting was encountered for both the left and right horizontal stabilizers. The buffeting increments were converted to coefficient form by the expression

$$\Delta C_{N_{T_B}} = \frac{\text{Load}}{qS_T}$$

where the load in this case is the double amplitude as measured from the strain-gage records. The data from each run were then plotted to obtain figure 5 on which $\Delta C_{N_{T_B}}$ is shown as a function of Mach number. Different symbols are used to separate the points for the left and right stabilizer and between intentional and "inadvertent" buffeting. Left-stabilizer points are shown as circles, right-stabilizer points as squares, and intentional-buffeting data are indicated with a cross superimposed on the left or right symbol. There is no noticeable difference in loads measured on the right or left tail.

The difference between the terms "inadvertent buffeting" and "intentional buffeting" is that in the case of inadvertent buffeting the pilot recovered quickly from the buffeting condition while for intentional buffeting the airplane was allowed to shake for a period of about 5 seconds. Inspection of figure 5 shows the inadvertent-buffeting loads to be, on the average, well below the intentional ones. This suggests that the length of time in buffeting may govern the magnitude of the buffet loads. Longer periods of time in buffeting may give the load components due to the various frequencies more of a chance to become in phase. Specifically, it can be seen from figure 5 that the buffeting-load increments measured in the abrupt pull-up maneuvers made at Mach numbers of 0.36, 0.40, and 0.45 are well below the maximum boundary. For these abrupt pull-ups, the pilot pushed down quickly as the airplane began to stall and thus, although higher lift coefficients were reached than during some gradual maneuvers in this same Mach number range, the loads are relatively low.

The test data are too limited to permit an accurate upper boundary to be faired through the data which may be used for extrapolation to other altitude or dynamic-pressure conditions. Longer periods in buffeting might have produced even larger loads. However the intentional-buffeting maneuvers are believed to be more severe than will normally be encountered on service airplanes and therefore the upper boundary should be conservative. Most of the data were obtained at 30,000 feet except for the point at $M = 0.23$ and $\Delta C_{N_{T_B}} = 0.26$ (absolute load value, ±1450 pounds) which was measured at a pressure altitude of 17,000 feet and is one of the points used in fairing the boundary line.

Using the boundary curve of figure 5 together with the expression

$$\frac{\Delta L_{T_B}}{2} = \Delta C_{N_{T_B}} q \frac{S_T}{2}$$

the variation of a maximum incremental buffeting structural tail load as a function of Mach number and pressure altitude was calculated and is shown in figure 6. These loads apply to one side of the tail outboard of the strain-gage station and represent the positive or negative increment in structural tail load about the balancing load. Curves are given for altitudes of 0, 10,000, 20,000, 30,000, and 40,000 feet pressure altitude. In order to define better the load limits for actual airplane operating conditions the curves of figure 4 have been cross plotted on figure 6 as lines of $n = 3$ and $n = 1$. The shaded area therefore represents buffeting conditions which cannot be reached without exceeding 3g. It will be noted that with 3g as a limit (3g equals limit load factor for the airplane design gross weight of 82,600 pounds) the maximum buffeting-load increments will occur at Mach numbers from 0.4 to 0.5 at pressure altitudes from 0 to 10,000 feet. Two points shown as circles are the points measured at 30,000 feet. The point at a Mach number of 0.48 and a load of ±2160 pounds is the largest shear increment measured.

According to information received from the manufacturer, the limit up load for the stabilizer per side was 9,250 pounds, while the limit down load for the stabilizer was -12,050 pounds per side. The stabilizer was loaded during static tests to 150 percent of the limit up load without failure and 157 percent of the limit down load before failure.

Although the maximum total buffeting tail-load increment reaches about 75 percent of the limit-up-load value, local stresses in the spar webs may be appreciably higher since one of the modes of vibration of the tail in buffeting is a torsional one and the strain-gage circuits are designed to nullify any torsion effects. Just what the stress increment due to torsion is for this airplane cannot be determined, but unreported tests made on an F-51D airplane at Langley with individual and combined strain-gage recording during buffeting indicates that torsional loads may double the load or stress in the spar webs.

Figure 7 is a plot of the horizontal-tail aerodynamic balancing load per side as a function of Mach number and pressure altitude. The curves for the various altitudes are the tail load (same as stabilizer load in this case) required to balance the airplane at the buffet boundary with the center of gravity at 30.5 percent M.A.C. They are determined from an unreported analysis of NACA flight tail-load measurements for the test airplane at 30,000, 22,500, and 15,000 feet. They are not exact since the calculations were made assuming a constant average aerodynamic-center position while the flight data indicated a forward movement of the aerodynamic center with increasing airplane normal-force coefficient. As on figure 6, the lines for $n = 3$ and $n = 1$ g airplane normal accelerations are for a weight of 82,600 pounds. The shaded region requires more than 3g to reach buffeting. At Mach numbers above about 0.75 the region requiring more than 3g lies between the $n = 3$ curve and the zero altitude curve.

Considering figures 6 and 7 together, it may be seen that the limit structural tail load could be exceeded in a gradual turn to 3g at a Mach number of 0.4 at sea level. The load per side would be 6500 pounds, buffeting increment, plus 4500 pounds, aerodynamic balancing, minus 1350 pounds, normal inertia, or a total of 9650 pounds. If the airplane were accelerating in pitch, this load would be exceeded. The term -1350 pounds arises from the normal inertia load on the tail in a turn to 3g, the weight of the tail outboard of the strain-gage station being 450 pounds.

Stabilizer bending moment.- The increments in the stabilizer bending-moment coefficient during buffeting are shown in figure 8 as a function of Mach number. As in the case of the tail shear, different symbols are used to separate intentional and inadvertent buffeting and left- and right-side values. The bending-moment coefficient is defined as

$$\Delta C_{BM_{T_B}} = \frac{\text{Bending moment}}{qS_T \frac{b_T}{2}}$$

where the bending moment is the double amplitude considering only the portion of the bending moment measured by the bending-moment bridge on either the left or right sides. There is no significant difference between the points shown for the left and right stabilizers, but intentional buffeting produces higher bending-moment increments than inadvertent buffeting. The highest bending-moment increment measured corresponds to the point shown at $M = 0.23$ and $\Delta C_{BM_{T_B}} = 0.124$ with an absolute value of ±176,000 inch-pounds.

Wing bending moment.- Left- and right-wing-buffeting bending-moment coefficients are plotted in figure 9 as a function of Mach number. The wing bending-moment coefficient is defined as

$$\Delta C_{BM_{W_B}} = \frac{\text{Bending moment}}{qS_W \frac{b_W}{2}}$$

where the bending moment is a double-amplitude measurement for the wing in buffeting. No distinction is made for left- and right-wing points or for intentional and inadvertent buffeting. No significant difference was found to exist for the two wings and bending moments in inadvertent maneuvers were lower than in intentional maneuvers. The highest bending-moment buffeting increment measured was at a Mach number of 0.23, a $\Delta C_{BM_{W_B}}$ of 0.036 with an absolute value of ±430,000 inch-pounds. Wing-buffeting bending-moment increments were determined from only the strain-gage bending-moment bridges on the wings.

No values of wing-shear buffeting increments are presented since the loads were always lower than ±1000 pounds and the shear-gage sensitivities for the wing only permits reading accuracies of ±400 pounds. For normal-maneuvering flight, the aerodynamic and inertia loads on the wing (for the weight as flown, about 60,000 lb) are of the same order of magnitude. Since the measured wing shears in buffeting were very small, it appears as though the aerodynamic and inertia loads in buffeting are 180° out of phase and of the same order of magnitude.

Elevator loads.- The elevator buffeting-load increments were determined by the addition of the measured loads on the outer and inner sets of hinge brackets. As explained in the section "Instrumentation," the elevator structural loads were obtained from equations of the form

$$\text{Load (Elevator)} = A\delta_{outer} + B\delta_{inner}$$

Although the peak buffeting increments did not always occur on the outer and inner hinge brackets at the same time, they were seldom more than 200 pounds different. For ease, therefore, in presenting the results the assumption has been made that the peak loads did occur at the same time.

The left- and right-elevator buffeting-load coefficients for both inadvertent- and intentional-buffeting maneuvers are shown in figure 10 as a function of Mach number. The elevator load coefficient is defined as

$$\Delta C_{N_{E_B}} = \frac{\text{Load}}{qS_E}$$

where the load is the double amplitude for one elevator during buffeting. Again there is no definite difference in left and right loads, but loads obtained during intentional buffeting are considerably higher on the average than in the inadvertent cases.

A maximum line is drawn on figure 10 from which the curves shown in figure 11 of elevator buffeting-load increment per side for various Mach numbers and altitudes were derived. Since there is some doubt regarding the boundary for figure 10 below a Mach number of 0.40, the curves of figure 11 start at this point. Lines identifying normal accelerations of 1 g and 3g for an airplane weight of 82,600 pounds are also shown. The shaded area represents a buffeting region for which the limit load factor of 3g would have to be exceeded.

The design limit up load for the elevator is 3675 pounds per side while the design limit down load is -4620 pounds per side. The elevator is reported by the manufacturer to have carried 187 percent of the limit up load and 150 percent of the limit down load without failure. While it appears as though the ultimate load for the elevator could easily be exceeded due to buffeting alone, there are several factors which make such a conclusion rather unlikely.

As mentioned previously, loads are being measured on the hinge-bracket supports and it is not possible to separate out for buffeting conditions the portion of the load on these brackets which is due to bending of the stabilizer and the actual load on the elevator. Even if most of the load on the hinges were coming from the elevator, a large portion of it may be due to the inertia of the large concentrated weight items (the mass balances) which would affect only the torque tube and the hinge-bracket stresses. If such were the case then, with the design margins of safety, the hinge brackets are more than adequate to carry these loads. The strain-gage instrumentation does not permit further analysis of this point.

The maximum measured elevator buffeting-load increment was ±2,750 pounds on the right side at a Mach number of 0.484 at a pressure altitude of 30,000 feet. This point, together with several others, is illustrated in figure 11. This buffeting load (2,750 pounds) is a larger load than the maximum buffeting load measured (2080) on the right stabilizer. This discrepancy can be due to omission of terms in computing the stabilizer shear or to the fact that elevator and stabilizer loads are not in phase at all times.

Buffeting and Structural Frequencies

As in the case of the tests reported in reference 6, there is a marked similarity between the structural natural frequencies and the frequencies which appear to be present in the strain-gage records. Table II lists some pertinent airplane structural frequencies obtained for the most part from vibration tests conducted on an XB-45 airplane at Wright-Patterson Air Force Base (reference 7). Since the tail span is longer by several feet than the one tested by the Air Force, the tail bending frequency listed was obtained in ground tests at the Langley Aeronautical Laboratory.

No detailed analysis has been made of the strain-gage records from a frequency standpoint mainly because the film speed was quite low, but a survey of all buffeting records showed the frequencies listed in the lower portion of table II. The frequencies are grouped with the strain-gage record from which they were obtained. The wing-bending gages showed a frequency very close to 4 cycles per second with occasional low-amplitude oscillations near 10 and 14 cycles per second. The stabilizer, shear, and bending strain-gage records were composed mainly of oscillations at 4, 6, 10, and 36 cycles per second. The elevator-shear-gage records were mainly composed of oscillations at 6 and 36 cycles per second. Some of the frequencies listed may be observed in the sample strain-gage record shown in figure 2, but the buffeting amplitudes are fairly low and it is difficult to pick out the high-frequency oscillations on this particular record.

During all buffeting maneuvers the wings were oscillating in phase, but the left- and right-elevator and stabilizer loads would be out of phase as often as in phase.

SUMMARY OF RESULTS

The gradual-stall buffet boundary, as established by the onset of buffeting from strain-gage records, appears similar to that of other airplanes with low-drag airfoils.

Maximum values of buffeting-load increments resulted from the intentional-buffeting maneuvers where buffeting continued for a considerable time. Smaller load increments were obtained during inadvertent buffeting where the time in buffeting was very short due to quick recovery.

The maximum buffeting tail-shear increment measured was ±2,160 pounds at a Mach number of 0.48 and a pressure altitude of 30,000 feet. The data indicated buffeting tail-load coefficients would decrease with increases in Mach number in the ranges investigated. Apparently, critical values of buffeting tail load may result at low altitudes and relatively low Mach numbers in gradual turns.

The maximum buffeting elevator load measured was ±2,750 pounds at a Mach number of 0.48 and a pressure altitude of 30,000 feet. While the extrapolation of the data has been limited to a Mach number range from 0.40 to 0.80, the data indicate loads measured on the elevator hinges could exceed the permissible limit load for the elevator within the present operating range of the airplane.

Wing bending moment and shear increments during buffeting were relatively small. The wing-shear increments never exceeded ±1000 pounds.

The buffeting frequencies estimated from the strain-gage records indicated a definite similarity to the structural natural frequencies. The left and right elevator and stabilizer were at times in phase and at times out of phase with one another, whereas the left and right wings were always in phase with one another during buffeting.

Langley Aeronautical Laboratory
National Advisory Committee for Aeronautics
Langley Field, Va.

REFERENCES

1. Aiken, William S., Jr., and Wiener, Bernard: Time Histories of Horizontal-Tail Loads on a Jet-Powered Bomber Airplane in Four Maneuvers. NACA RM L9H16a, 1949.

2. Cooney, T. V., and McGowan, William A.: Time Histories of Loads and Deformations on a B-45A Airplane in Two Aileron Rolls. NACA RM L9I28a, 1949.

3. Cooney, T. V., and Aiken, William S., Jr.: Time Histories of the Loads and Deformations on the Horizontal Tail on a Jet-Powered Bomber Airplane in Accelerated Maneuvers at 30,000 Feet. NACA RM L50B24a, 1950.

4. McGowan, William A., and Wiener, Bernard: Time Histories of Horizontal Tail Loads and Deformations on a Jet-Powered Bomber Airplane during Wind-Up Turns at 15,000 Feet and 22,500 Feet. NACA RM L50C21a, 1950.

5. McGowan, William A.: Time Histories of Horizontal-Tail Loads, Elevator Loads, and Deformations on a Jet-Powered Bomber Airplane during Wind-Up Turns at Approximately 15,000 Feet and 22,500 Feet. NACA RM L50F28, 1950.

6. Stokke, Allen R., and Aiken, William S., Jr.: Flight Measurements of Buffeting Tail Loads. NACA TN 1719, 1948.

7. Mykytow, Walter J.: Vibration Inspection and Flutter Analysis of the North American XB-45 Airplane. Air Materiel Command, Army Air Forces, ser. No. TSEAC 5-4262-25-34, May 20, 1947.

TABLE I

GEOMETRIC CHARACTERISTICS OF TEST AIRPLANE

Wing:	
Span, feet	89.04
Area, square feet	1175
Mean aerodynamic chord, feet	14.02
Airfoil, root	NACA 66,2-215
Airfoil, tip	NACA 66,1-212
Taper ratio	2.42
Horizontal Tail Surfaces:	
Area (including fuselage), square feet	289.44
Span, feet	43.87
Elevator:	
Area (including tabs), square feet	67.71

NACA

TABLE II

FREQUENCY CHARACTERISTICS

Natural Frequencies of Airplane Components (cps):	
Wing:	
First symmetrical bending	4.6
First antisymmetrical bending and inner-pannel torsion	5.2
Symmetric bending and inner-panel torsion	6.2
Unsymmetrical wing bending and inner-panel torsion	9.2
Second symmetrical bending	14.3
Outer-panel torsion	25.3
Fuselage, torsion and side bending (primarily torsion)	4.3
Fuselage vertical bending	8.0
Horizontal stabilizer:	
Primary bending (symmetrical)	6.7
Torsion	36.7
Elevator:	
Torque tube torsion	14.2
Symmetrical rotation	8.3 to 10.0
Buffeting Frequencies Estimated from Records for the Following Strain-Gage Bridges (cps):	
Wing bending	4, 10, 14
Stabilizer shear	4, 6, 10, 36
Stabilizer bending	4, 5, 6, 10, 36
Elevator shear	6, 36

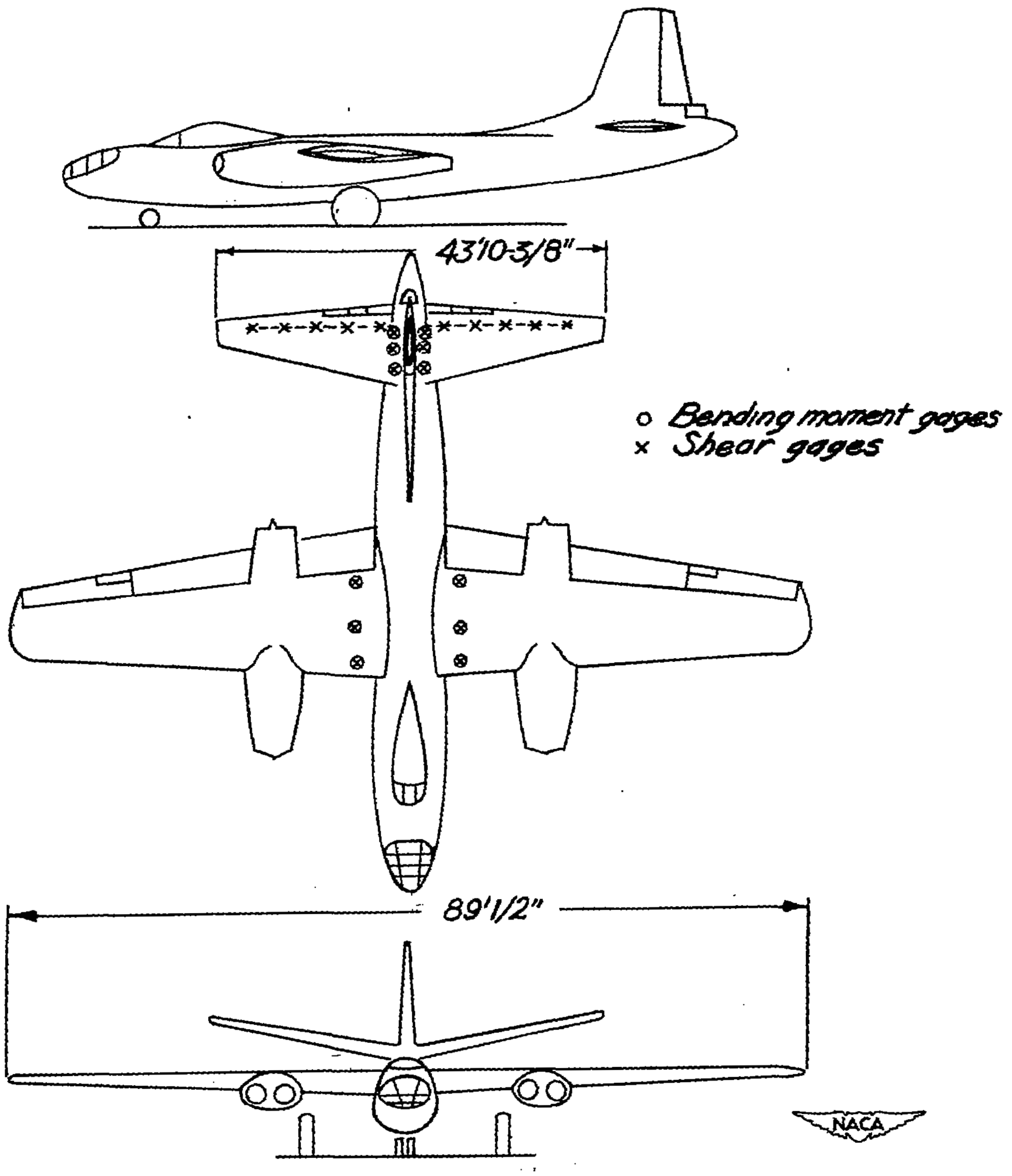

Figure 1.- Three-view drawing of test airplane showing approximate locations of strain-gage bridges.

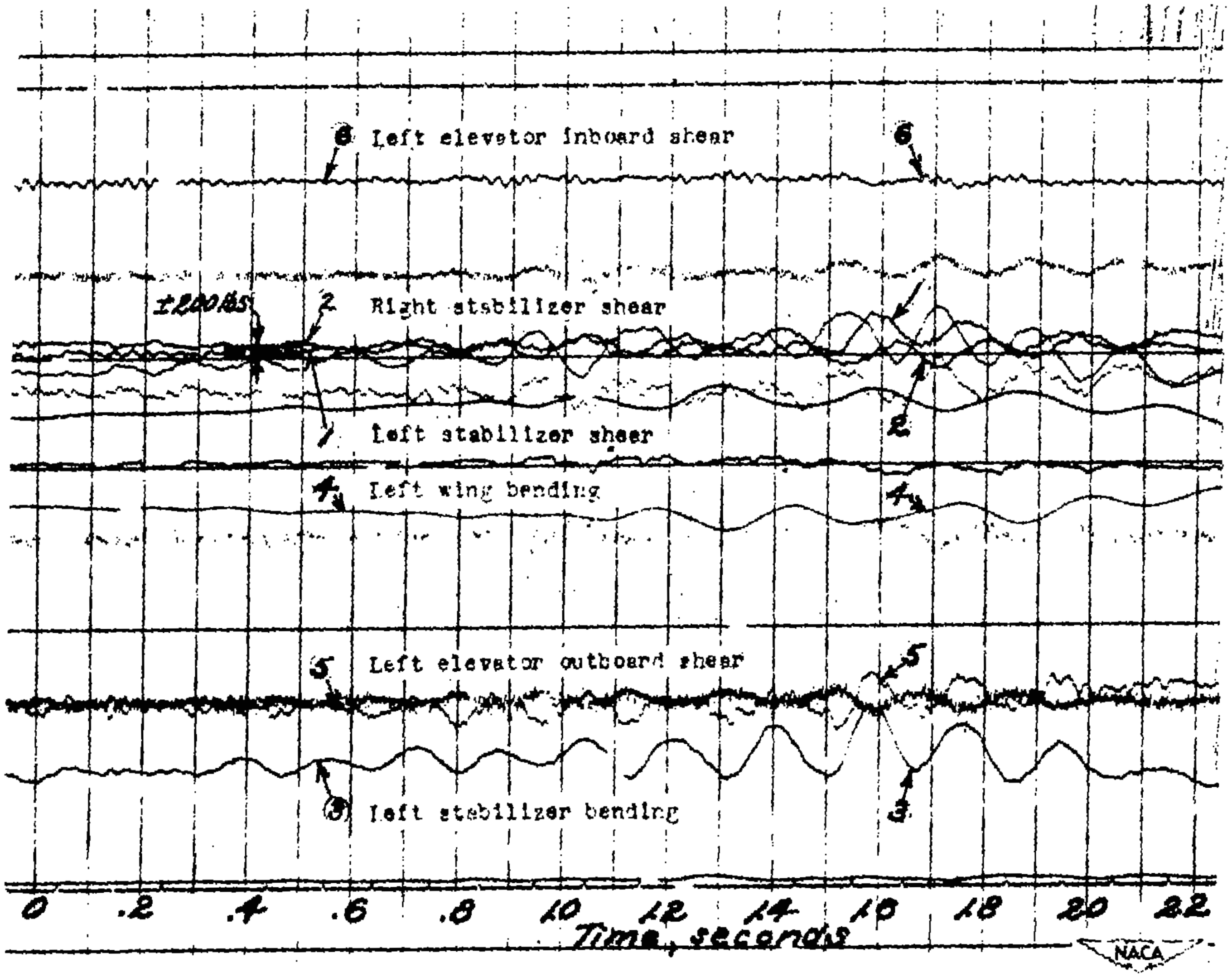

Figure 2.- Typical strain-gage record during buffeting.

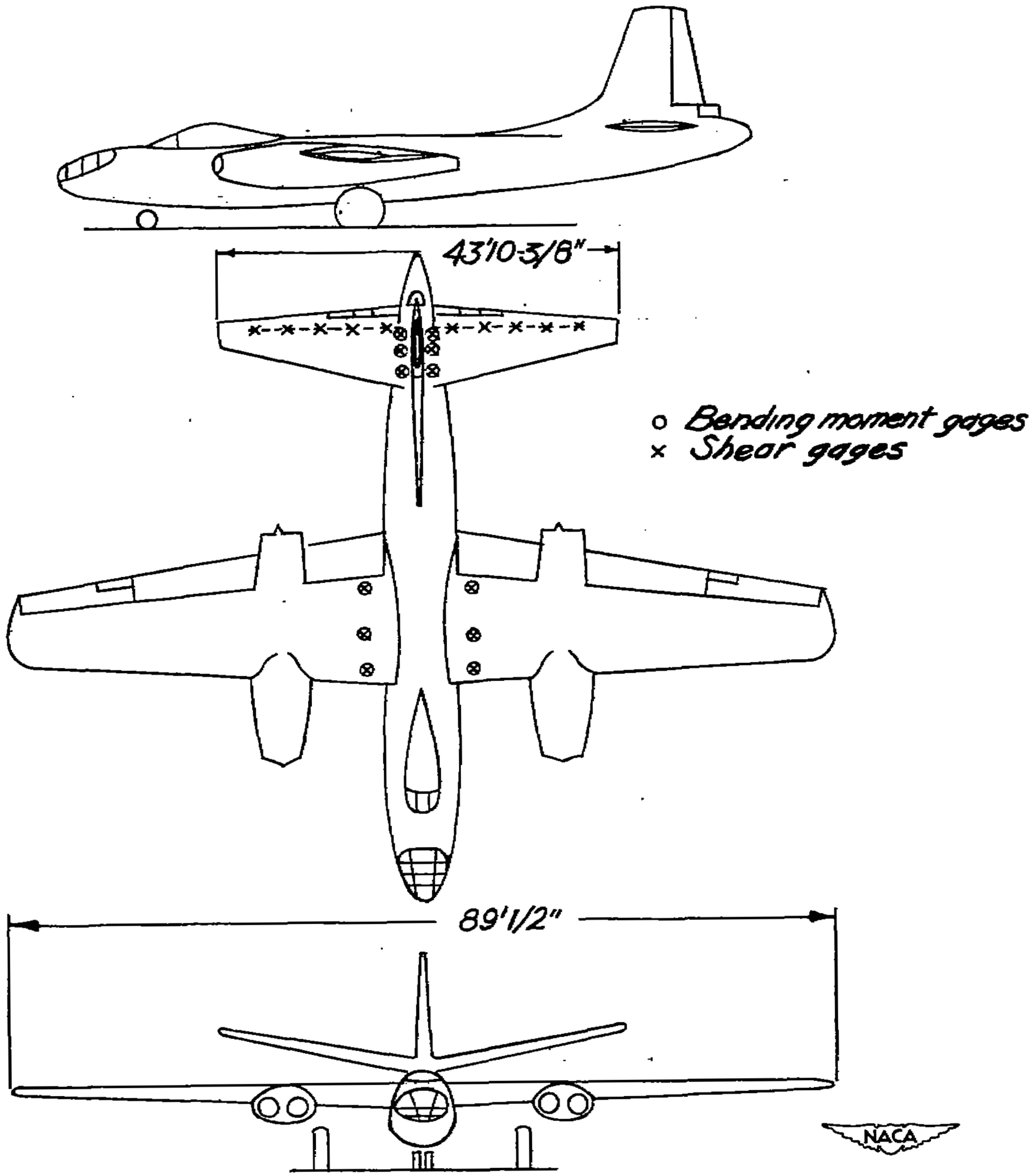

Figure 1.- Three-view drawing of test airplane showing approximate locations of strain-gage bridges.

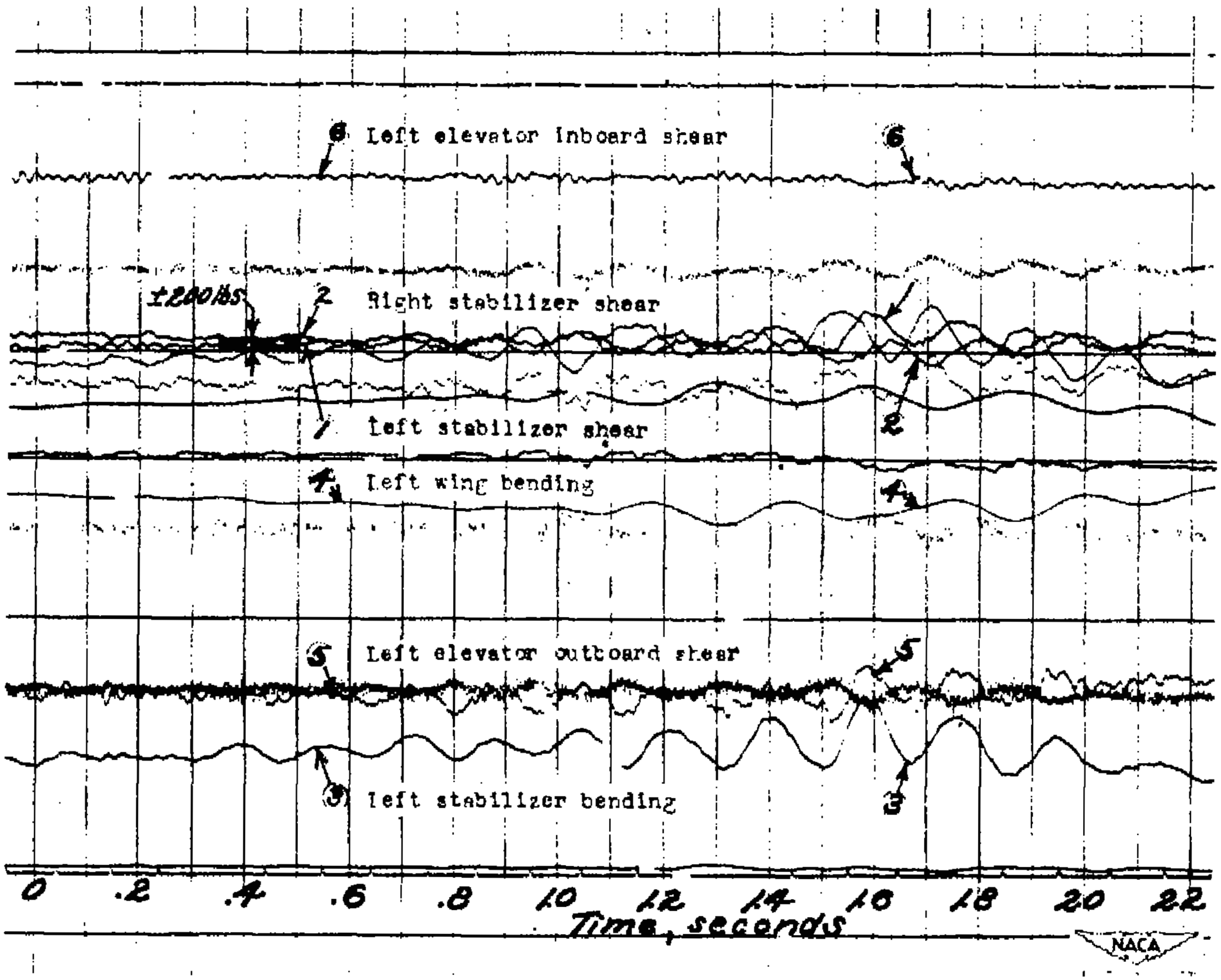

Figure 2.- Typical strain-gage record during buffeting.

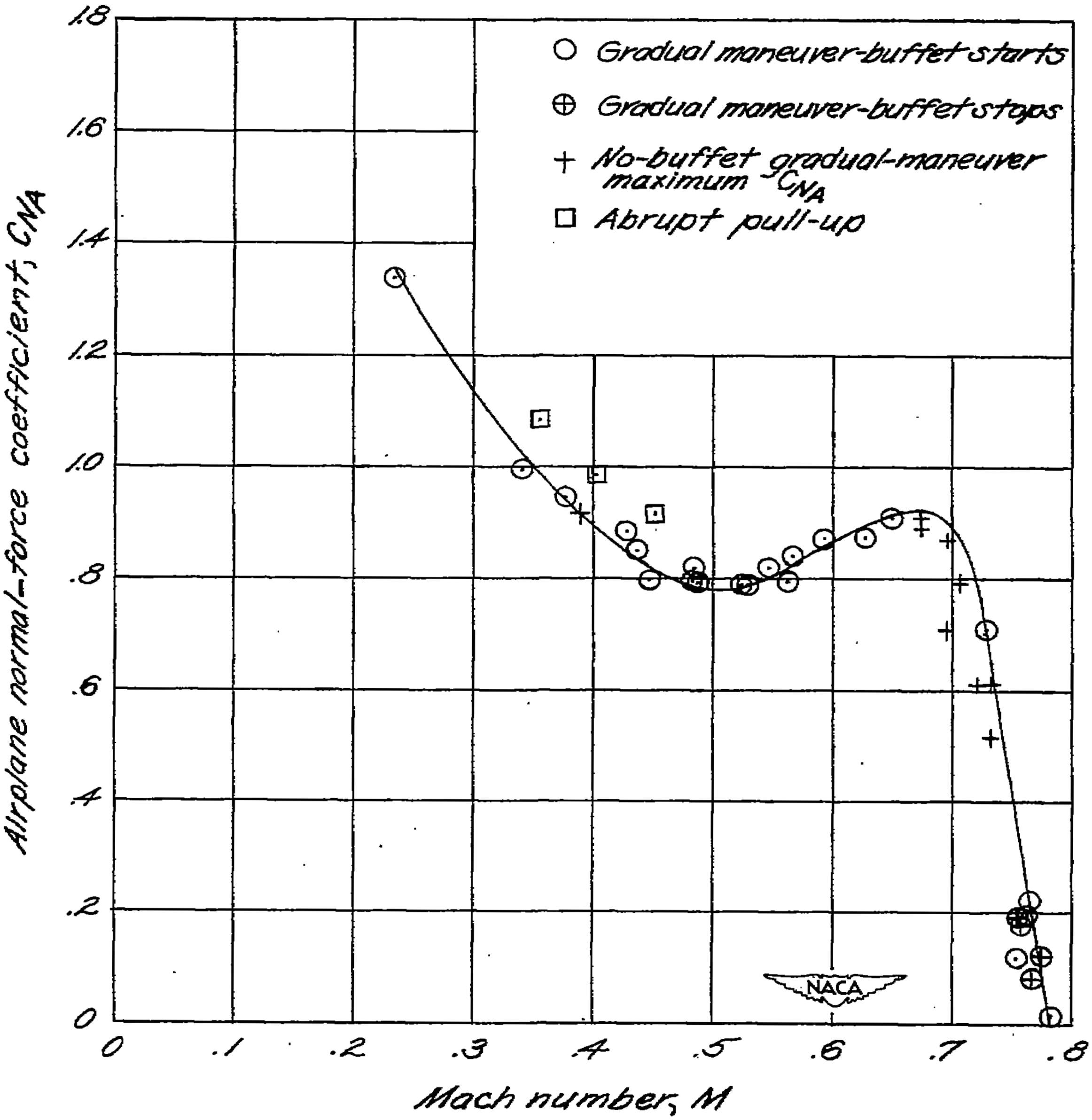

Figure 3.- Buffet boundary for test airplane.

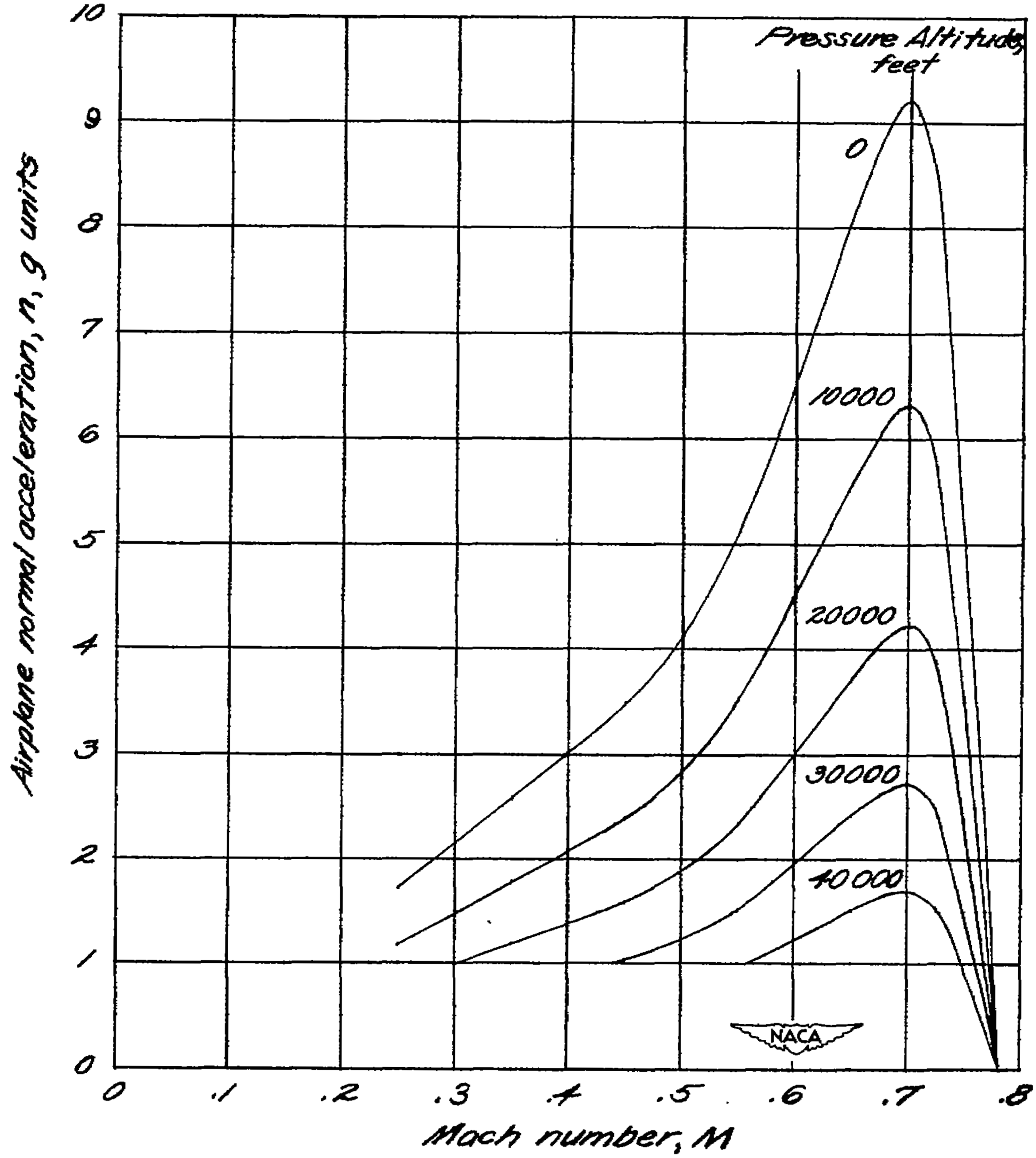

Figure 4.- Gradual-turn buffet boundaries for test airplane at design weight = 82,600 pounds.

[redacted]

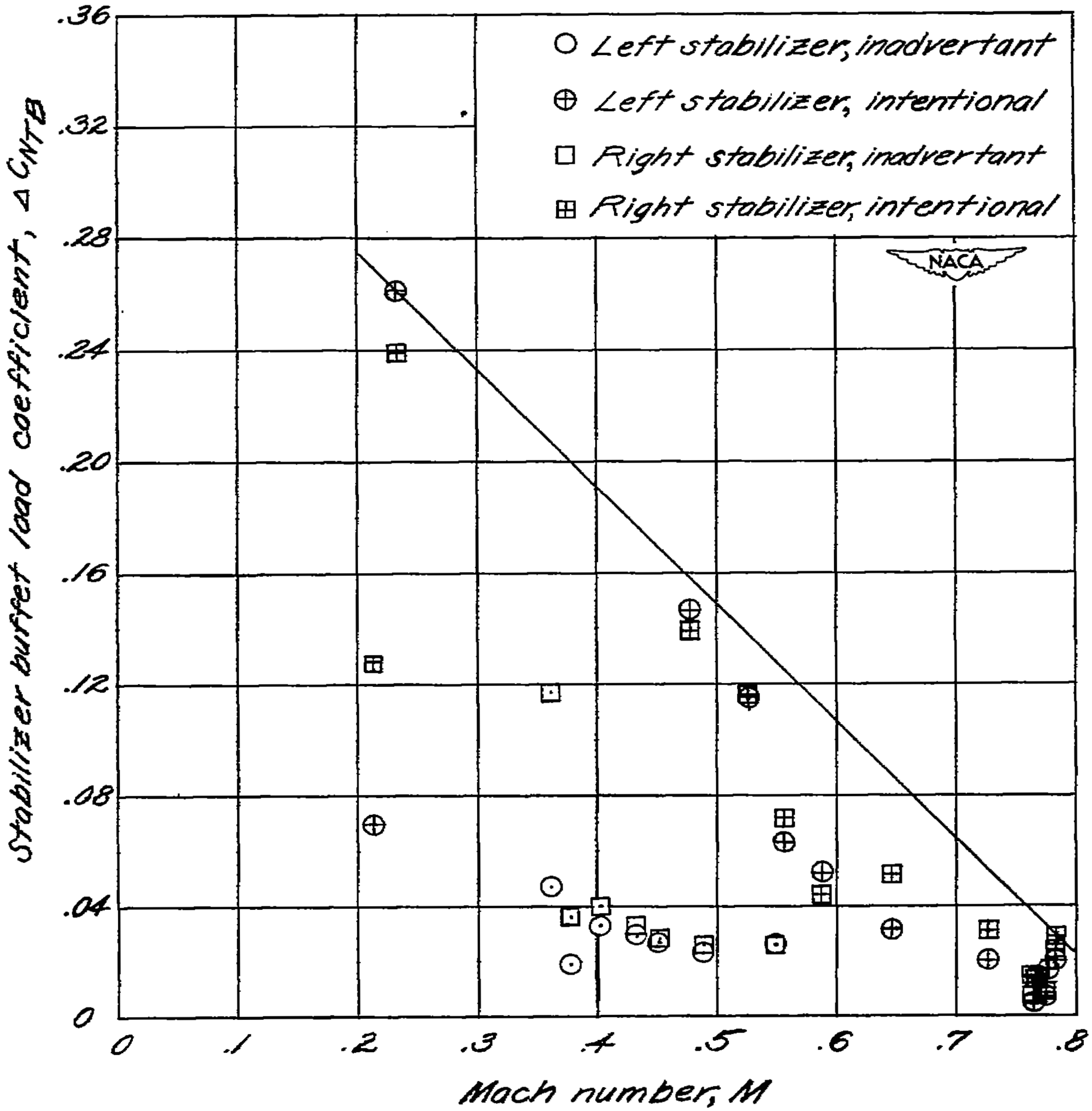

Figure 5.- Stabilizer buffeting-load coefficients for test airplane.

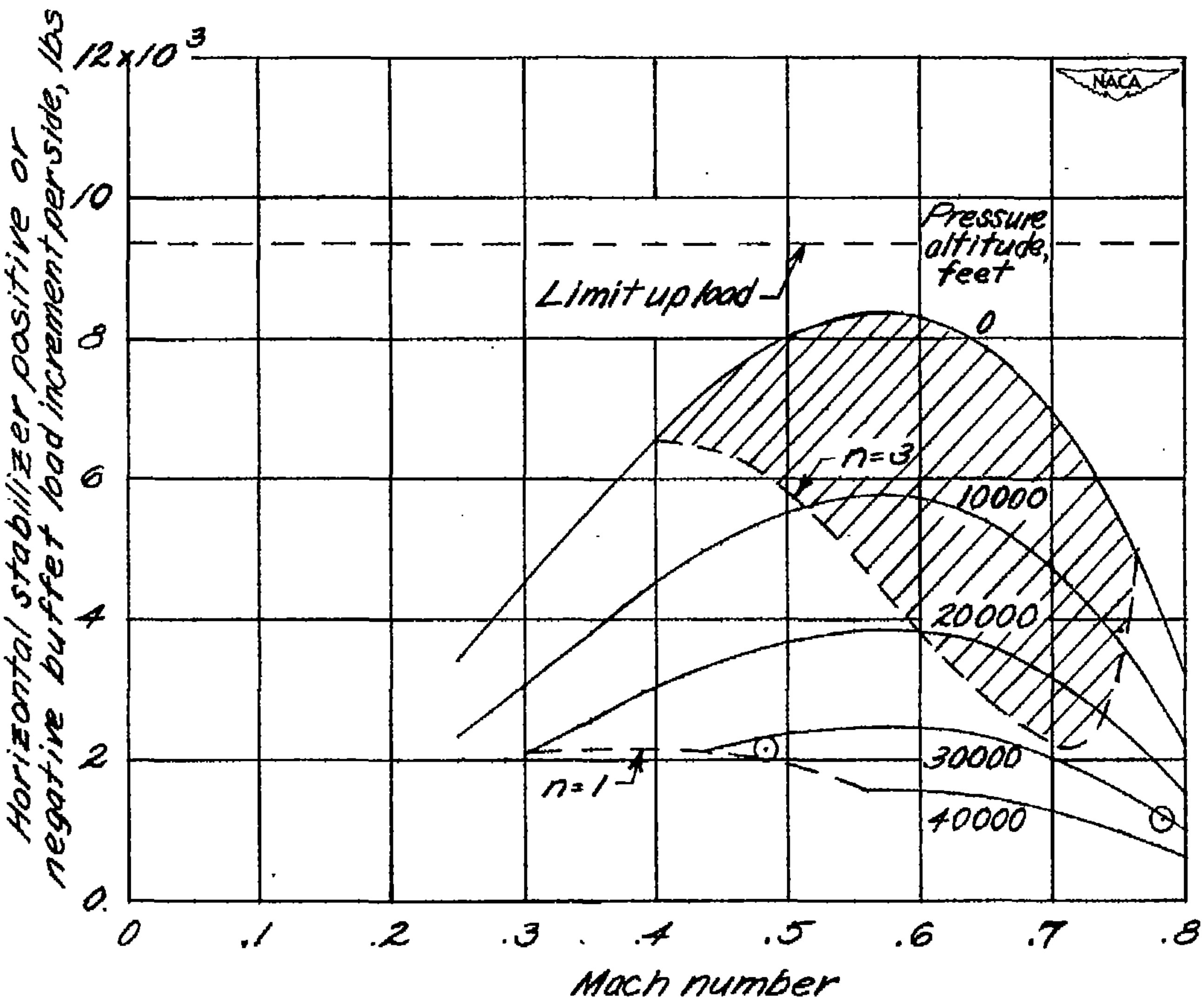

Figure 6.- Horizontal stabilizer buffeting-load increments per side for test airplane at various altitudes.

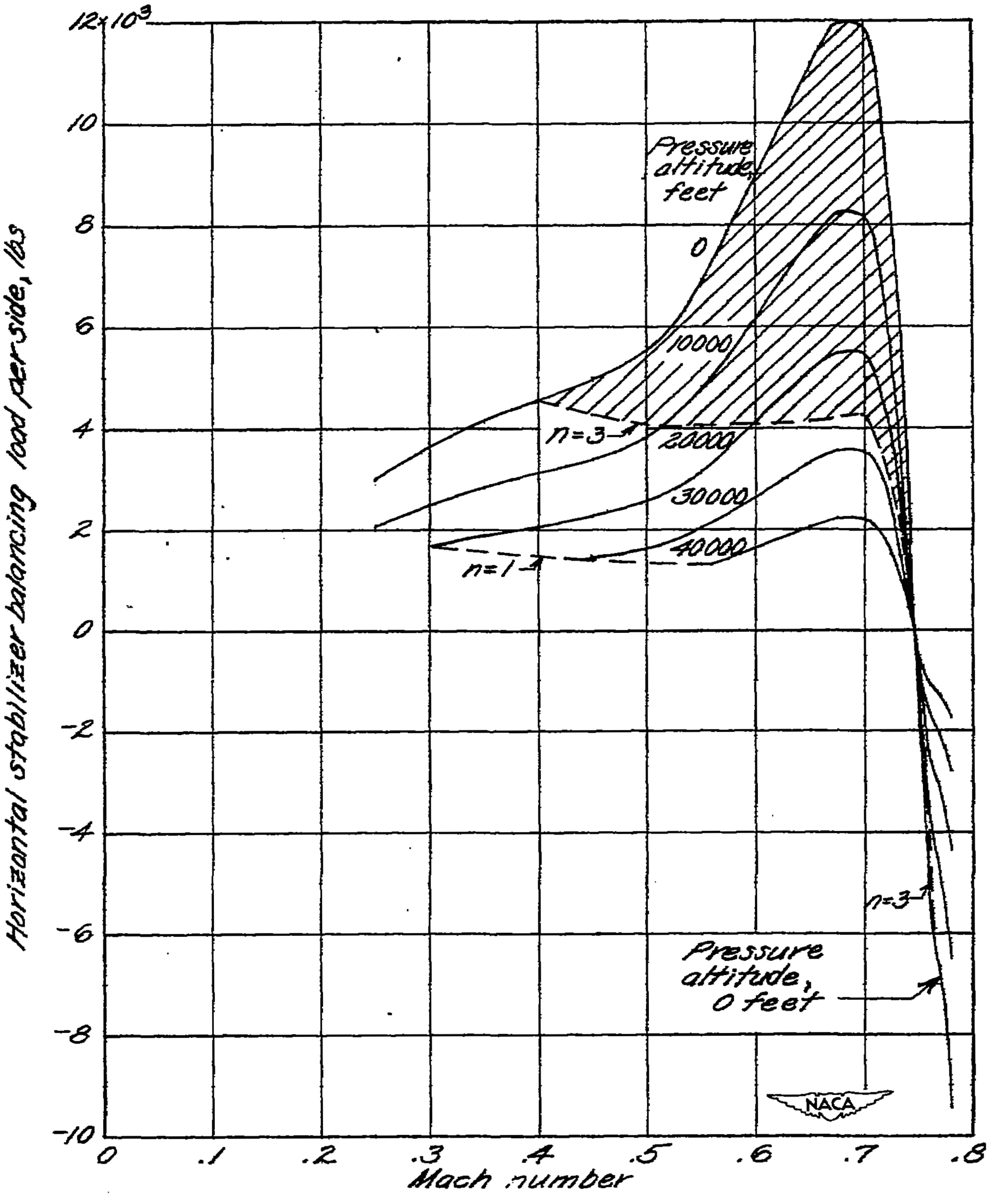

Figure 7.- Horizontal stabilizer balancing loads per side for test airplane at buffet boundary for various altitudes.

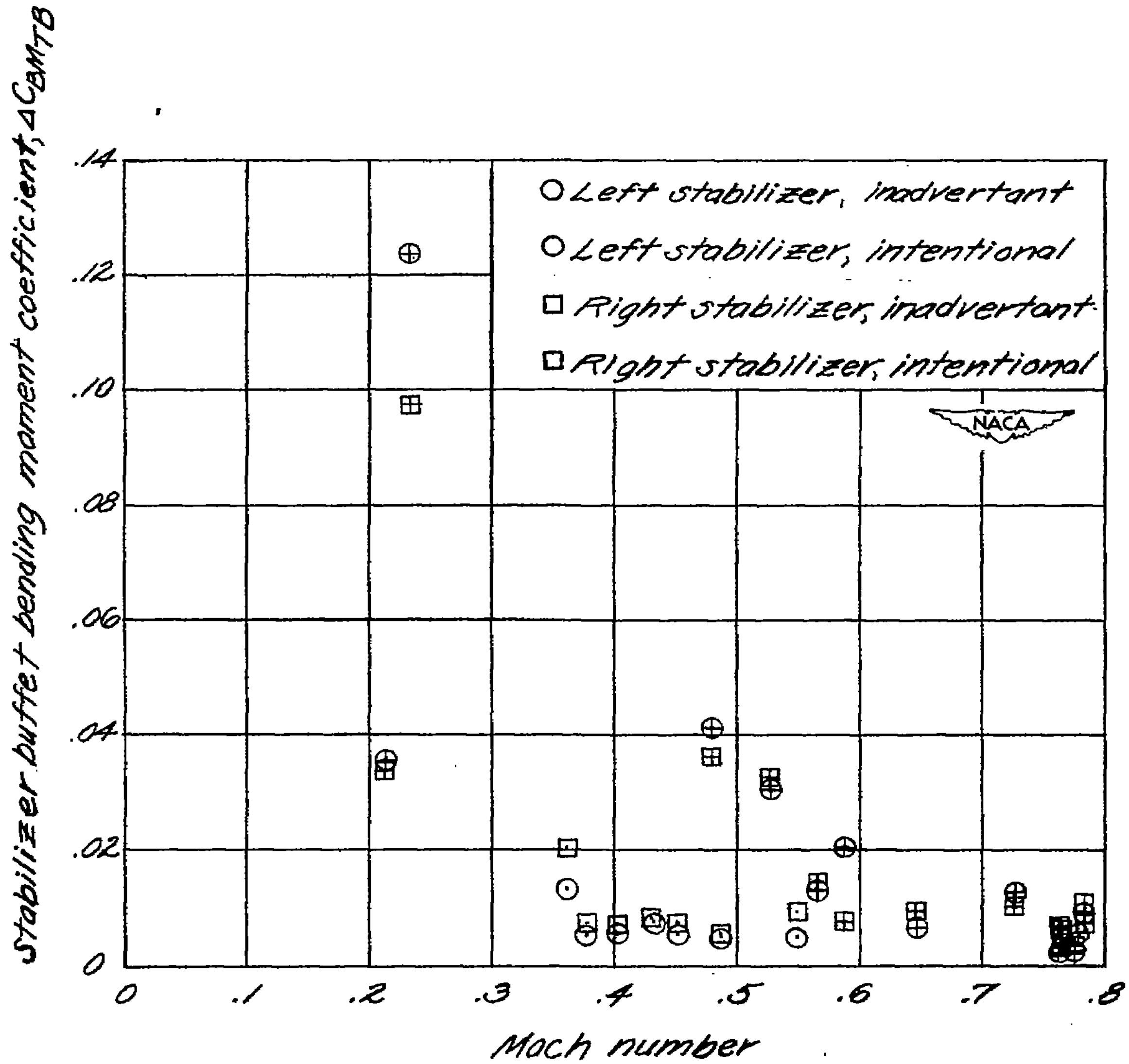

Figure 8.- Stabilizer buffeting bending-moment coefficients for test airplane.

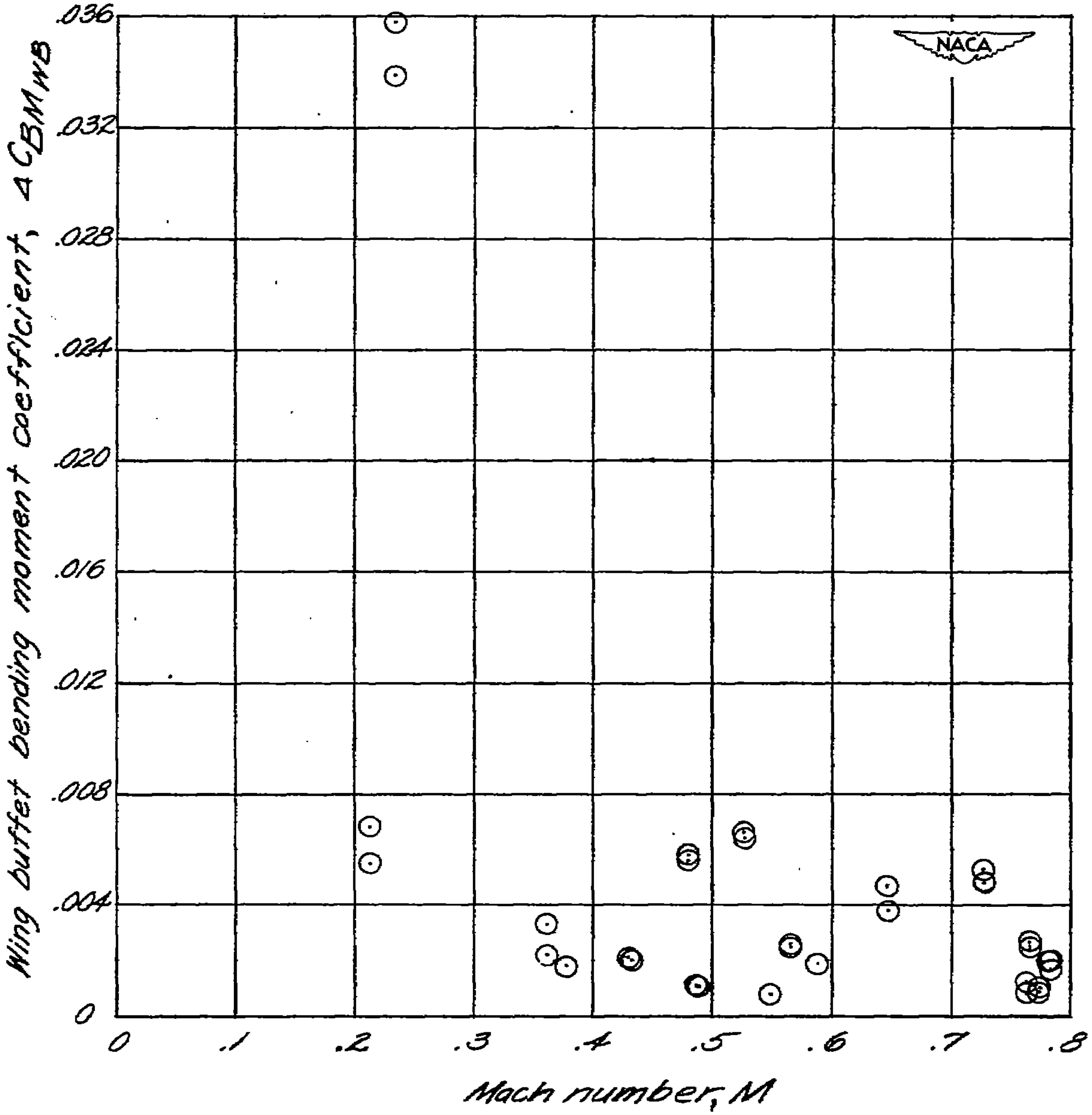

Figure 9.- Left- and right-wing buffeting bending-moment coefficients for test airplane.

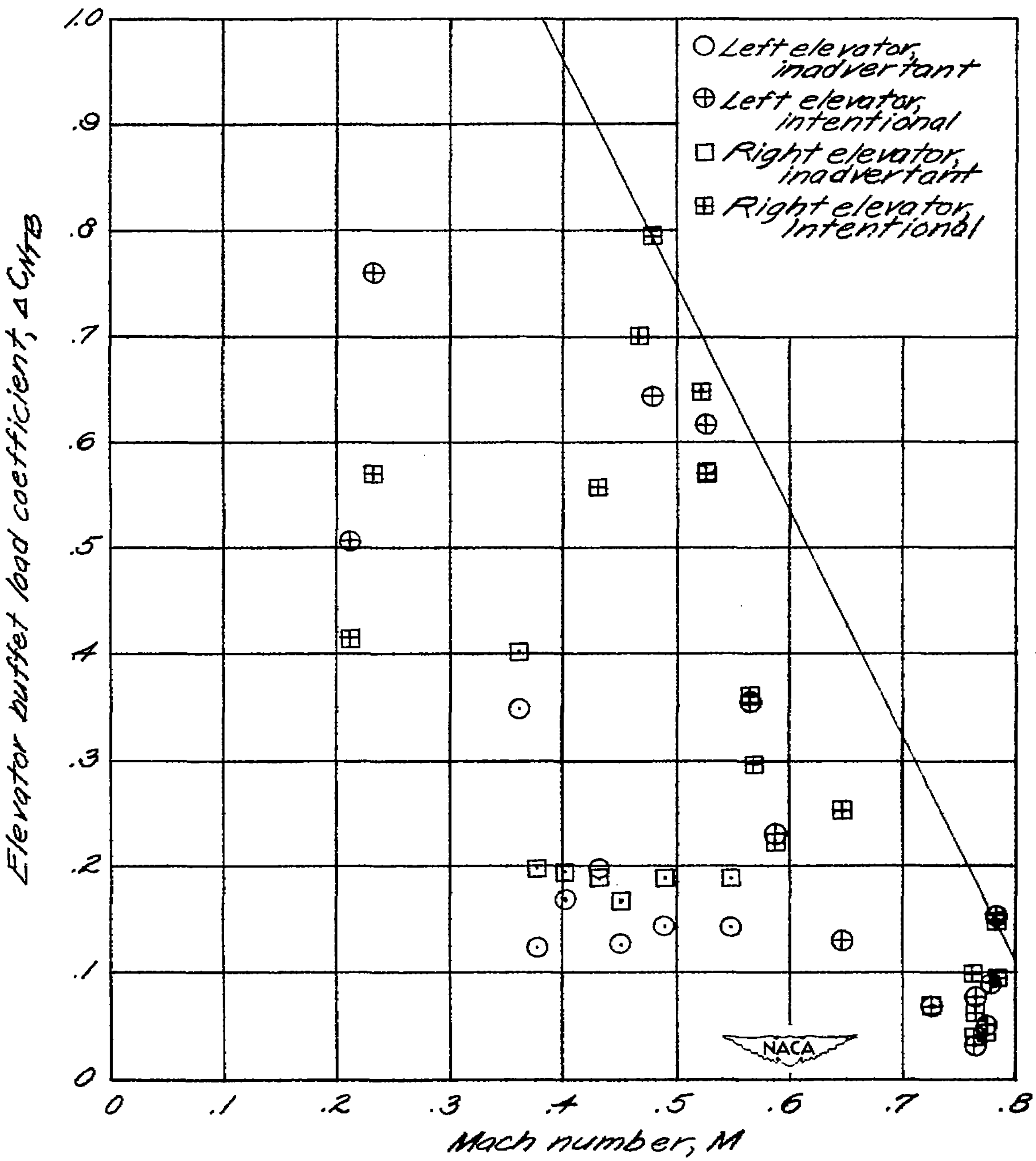

Figure 10.- Elevator buffeting-load coefficients for test airplane.

[redacted]

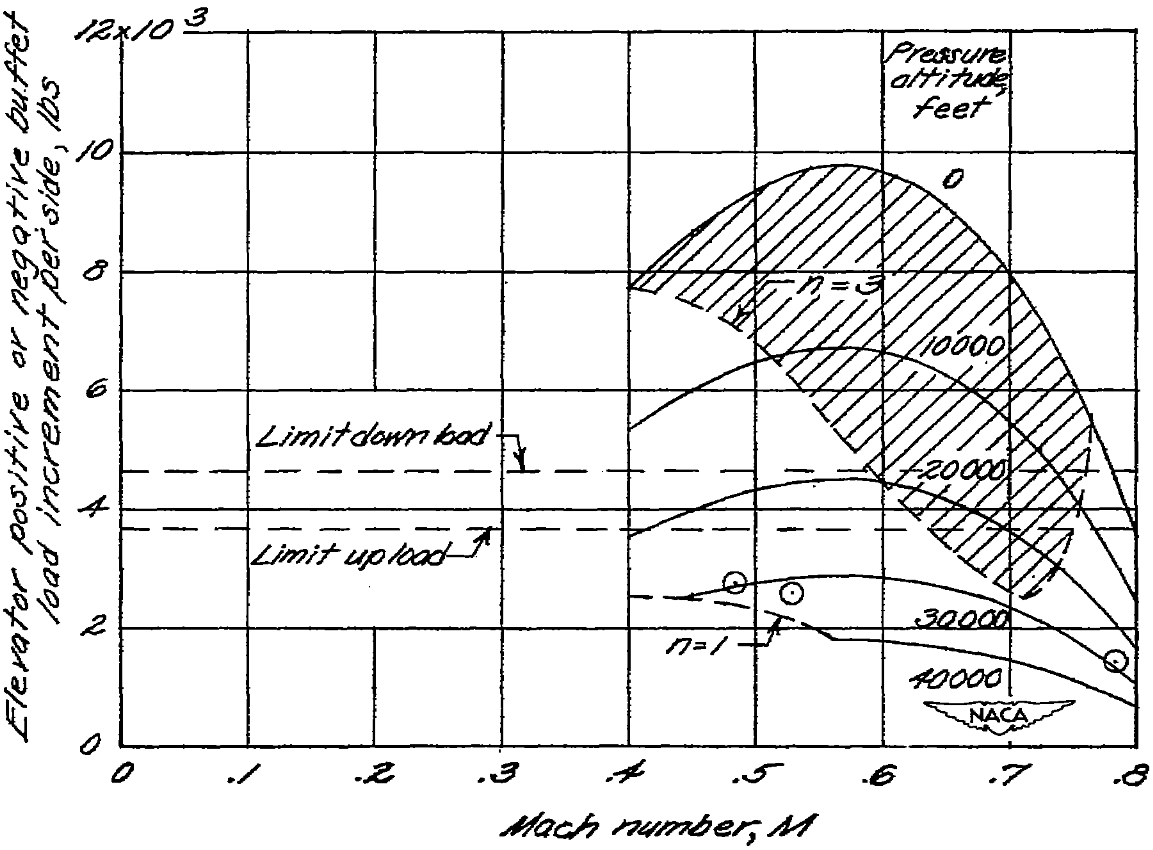

Figure 11.- Elevator buffeting-load increments per side for test airplane at various altitudes.